ELSEVIER

Journal of Photochemistry and Photobiology A: Chemistry 128 (1999) 15–25

Journal of Photochemistry and Photobiology A:Chemistry

www.elsevier.nl/locate/jphotochem

Kinetic study of the reactions of OH and OD with HBr and DBr

Y. Bedjanian *, V. Riffault, G. Le Bras, G. Poulet

Laboratoire de Combustion et Systèmes Réactifs, CNRS and Université d'Orléans, 45071 Orléans Cedex 2, France

Received 5 July 1999; accepted 26 July 1999

Abstract

The kinetics of the reactions of OH and OD radicals with HBr and DBr, OH + HBr (1), OD + HBr (3), OH + DBr (4) and OD + DBr (5), have been studied by the mass spectrometric discharge-flow method at temperatures between 230 and 360 K and at total pressure of 1 Torr of helium. The following Arrhenius expressions were obtained: $k_1 \approx k_3 = (5.3 \pm 1.2) \times 10^{-12} \exp\{(225 \pm 60)/T\}$ and $k_4 \approx k_5 = (4.3 \pm 1.2) \times 10^{-12} \exp\{(125 \pm 80)/T\}$ cm^3 s^{-1} per molecule. The isotope exchange reactions OD + HBr → OH + DBr (3′) and OH + DBr → OD + HBr (4′) were found to be slow and the upper limits for the rate constants of these channels were measured at $T = 298$ K: $k_{3'} < 1 \times 10^{-13}$ and $k_{4'} < 3 \times 10^{-14}$ cm^3 s^{-1} per molecule. These results are compared with the literature experimental and computational data.

Keywords: Reaction; Kinetics; Rate constant; OH; OD; HBr; DBr; Kinetic isotopic effect

1. Introduction

The reaction of OH with HBr is known to be of importance in stratospheric ozone chemistry as influencing the bromine partitioning between its active forms and reservoirs e.g. [1]:

$$OH + HBr \rightarrow Br + H_2O \quad (1)$$

The kinetics of this reaction has been previously investigated at room temperature [2–7] and as a function of temperature in the ranges $T = (249–416)$ K [8], (23–295) K [9] and (76–242) K [10]. The rate constant of reaction (1) has been found to be pressure independent e.g. [8–10], consistent with a bimolecular mechanism. At present, the value of the rate constant at room temperature can be considered as well established: $k_1 = (1.1 \pm 0.2) \times 10^{-11}$ cm^3 s^{-1} per molecule [11,12]. However, the value of k_1 at stratospheric temperatures remains somewhat uncertain. Recent compilations of kinetic data for atmospheric chemistry give different (although close) recommendations for the temperature dependence of k_1: $k_1 = (1.1 \pm 0.2) \times 10^{-11}$ (temperature independent) [11] and $k_1 = 1.1 \times 10^{-11}\ (T/298)^{-0.8}$ cm^3 s^{-1} per molecule over the temperature range 200–400 K [12].

In the present study, the kinetics of reaction (1) has been investigated in the temperature range between 230 and 360 K. The main motivation for this work was its relation to the study of the reaction between OH and BrO, which is currently being carried out in this laboratory:

$$OH + BrO \rightarrow HO_2 + Br \quad (2a)$$

$$OH + BrO \rightarrow HBr + O_2 \quad (2b)$$

The potential occurrence of channel (2b) is of great importance for the stratospheric bromine partitioning [13,14]. Hence, the experimental determination of the branching ratio for channel (2b) is required. From the unique study of reaction (2) [15], and considering that the branching ratio of channel (2b) is likely to be as low as a few percents, it appears that one cannot neglect the side and secondary processes involved in the reactive system used to produce OH and BrO radicals. Thus, accurate kinetic data for all these reactions are needed. In this aim, the kinetic parameters for the reactions of OH and OD with Br_2 [16] and for the disproportionation reactions of OH and OD radicals [17] have already been reported recently. Accurate kinetic information on reaction (1) between OH and the possible minor product HBr is also needed. Isotopic substitution is known to be adapted from kinetic studies, especially for the determination of reaction products yields. Hence, in order to provide a complete dataset for all the isotopic variants of reaction (1), the following reactions have been also investigated:

$$OD + HBr \rightarrow Br + HOD \quad (3)$$

$$OH + DBr \rightarrow Br + HOD \quad (4)$$

* Corresponding author. Tel.: +33-2-38255474; fax: +33-2-38257905
E-mail address: bedjanian@cnrs-orleans.fr (Y. Bedjanian)

1010-6030/99/$ – see front matter
PII: S1010-6030(99)00159-8

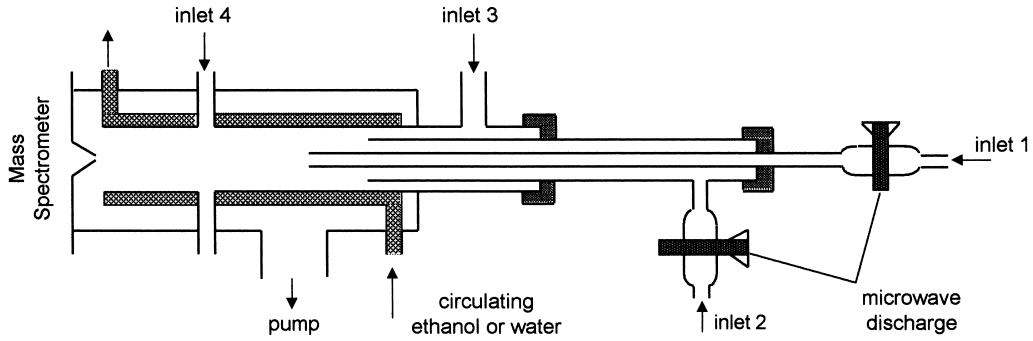

Fig. 1. Diagram of the apparatus used.

$$OD + DBr \rightarrow Br + D_2O \quad (5)$$

Besides, kinetic data for these reactions have a fundamental interest, because these relatively simple chemical systems are appropriate for theoretical calculations, thus, for testing different theories of reaction rates. The OH + HBr reaction has already been a subject of theoretical calculations [18–20], which will be discussed from the comparison with the present experimental data.

2. Experimental

Experiments were carried out in a discharge flow reactor using a modulated molecular beam mass spectrometer as the detection method. The main reactor, shown in Fig. 1 along with the movable injector for the reactants, consisted of a Pyrex tube (45 cm length and 2.4 cm i.d.) with a jacket for the thermostated liquid circulation (water or ethanol). The walls of the reactor as well as of the injector were coated with halocarbon wax in order to minimize the heterogeneous loss of active species. All experiments were conducted at 1 Torr total pressure, helium being used as the carrier gas.

The fast reaction of hydrogen atoms with NO_2 was used as the source of OH radicals, H atoms being produced in a microwave discharge of H_2/He mixture:

$$H + NO_2 \rightarrow OH + NO \quad (6)$$

$k_6 = 4.0 \times 10^{-11} \exp(-340/T)\ cm^3\ s^{-1}$ per molecule [11]

Similarly, the reaction of D atoms with NO_2 was used to produce OD radicals:

$$D + NO_2 \rightarrow OD + NO \quad (7)$$

$k_7 = (1.20 \pm 0.25) \times 10^{-11}\ cm^3\ s^{-1}$ per molecule (T = 230–365 K) [17]

NO_2 was always used in excess over H and/or D atoms. Generally, OH and OD radicals were detected as $HOBr^+$ (m/e = 96/98) and $DOBr^+$ (m/e = 97/99), respectively, after scavenging by an excess of Br_2 (added at the end of the reactor through inlet 4, located 5 cm upstream of the sampling cone) via reactions (8) and (9), respectively:

$$OH + Br_2 \rightarrow Br + HOBr \quad (8)$$

$k_8 = (1.8 \pm 0.3) \times 10^{-11} \exp\{(235 \pm 50)/T\}\ cm^3\ s^{-1}$ per molecule [16]; $k_8 = (1.98 \pm 0.51) \times 10^{-11} \exp\{(238 \pm 70)/T\}\ cm^3\ s^{-1}$ per molecule [21]

$$OD + Br_2 \rightarrow Br + DOBr \quad (9)$$

$k_9 = (1.9 \pm 0.2) \times 10^{-11} \exp\{(220 \pm 25)/T\}\ cm^3\ s^{-1}$ per molecule [16].

This method for OH and OD detection was preferred to the direct detection of these radicals at m/e = 17 (OH^+) and m/e = 18 (OD^+), respectively, due to significant contributions of traces of water vapor at these peaks. The same procedure of OH (OD) chemical conversion to HOBr (DOBr) was used for the measurements of the absolute concentrations: $[OH] = [HOBr] = \Delta[Br_2]$ (or $[OD] = [DOBr] = \Delta[Br_2]$). Thus, OH (OD) concentrations were determined from the consumed fraction of $[Br_2]$. $[Br_2]$ was determined from the measured flow rate of known Br_2/He mixtures. The possible influence of secondary chemistry on this detection method of HOBr (DOBr) detection and their absolute calibration procedure was discussed in details in previous papers [16,17]. In a few experiments, OH and OD were directly detected at their parent peaks (m/e = 17 and 18, respectively) with extraction of the contribution of H_2O. This procedure was shown to give the same concentrations (within 5%) for OH and OD radicals as their titration by Br_2.

The absolute calibration of HBr (detected at its parent peaks m/e = 80/82) was made from the flow rate measurements of known HBr/He mixtures. This method to measure the absolute concentrations of HBr has to be applied with special care. It is known that HBr can decompose during its storage giving H_2 and Br_2, which can act as unknown diluent of the HBr e.g. [22,23]. In the present study, HBr (Aldrich, stated purity > 99.8%) was purified by distillation before use. HBr/He mixtures were stored in a glass flask which was previously passivated with HBr. It was verified by mass spectrometry (detection of the possible decomposition product Br_2 and invariance of the HBr calibration from day to day) that no significant decomposition of HBr was occurred during its storage for a few weeks. The decomposition product, Br_2, was measured to be less than 0.1%

of HBr. In order to verify, the reliability of these measurements of the HBr absolute concentrations, another method was used. It consisted of the chemical conversion of H atom to HBr by excess Br_2:

$$H + Br_2 \rightarrow Br + HBr \quad (10)$$

$k_{10} = 6.7 \times 10^{-10} \exp(-673/T)\ cm^3\ s^{-1}$ per molecule [24]

In this case, the concentration of HBr formed was determined from the fraction of Br_2 consumed. The results obtained by these two calibration methods were always in good agreement (within less than 10%).

Deuterium bromide, DBr, used in the present study, was in solution with D_2O, so that the DBr concentration in the reactor could not be determined from its flow rate. In all experiments, the same sensitivity was considered for HBr and DBr ($m/e = 81/83$). This was verified experimentally. Using the chemical conversion of H and D atoms to HBr and DBr via reactions (10) and (11), respectively, the intensity of both HBr and DBr signals could be related to the concentration of Br_2:

$$D + Br_2 \rightarrow Br + DBr \quad (11)$$

$k^{11} = 6.0 \times 10^{-10} \exp(-709/T)\ cm^3\ s^{-1}$ per molecule [24]

In a second series of experiments, HBr and DBr were titrated by excess H atoms in reactions (12) and (13), respectively:

$$H + HBr \rightarrow Br + H_2 \quad (12)$$

$k_{12} = 2.5 \times 10^{-11} \exp(-400/T)\ cm^3\ s^{-1}$ per molecule [25]

$$H + DBr \rightarrow Br + DH \quad (13)$$

$k_{13} = 4.1 \times 10^{-11} \exp(-650/T)\ cm^3\ s^{-1}$ per molecule [25]

In this case, the intensities of HBr and DBr signals could be related to the concentration of Br atoms formed in reactions (12) and (13). Fig. 2 shows an example of such a dependence of [Br] produced on the consumed concentrations of HBr and DBr. It can be seen that the ratio of concentration to signal intensity is the same for HBr and DBr.

The purities of the gases used were as follows: He > 99.9995% (Alphagaz), was passed through liquid nitrogen traps; H_2 > 99.998% (Alphagaz); D_2 > 99.7% (Alphagaz); Br_2 > 99.99% (Aldrich); NO_2 > 99% (Alphagaz); HBr > 99.8% (Praxair); DBr, 47 wt.% solution in D_2O (>99% atom D, Aldrich).

3. Results

3.1. Reactions OH + HBr (1) and OD + HBr (3)

Two types of experiments were carried out to measure the rate constants of the OH + HBr and OD + HBr reactions, either by monitoring the OH (OD) decay kinetics with an excess of HBr over OH (OD) or by monitoring the HBr decay kinetics with an excess of OH (OD) radicals.

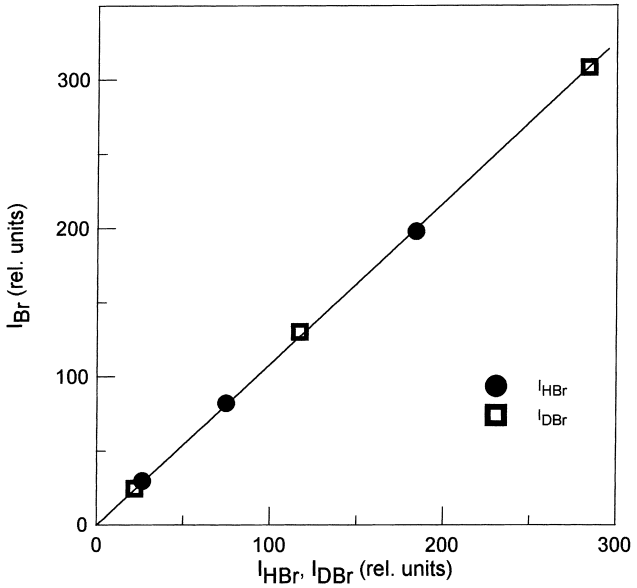

Fig. 2. Relative calibration of HBr and DBr signals: dependence of the concentration of Br atoms formed in reactions (12) and (13) versus concentrations of the consumed HBr and DBr (see text).

HBr is known to be a very sticky molecule, which could lead to heterogeneous complications in the study of HBr reactions under flow conditions, particularly at low temperatures. The first observation in the present study was that the kinetic measurements were not reliable at temperatures below 0°C. It was observed that the HBr addition in the reactor at low temperatures modified the reactor surface, giving irreproducible OH (OD) kinetics. Evidence for the heterogeneous reaction of OH with adsorbed HBr was found. On the contrary, in the study of the reaction of OH and OD with DBr, no heterogeneous complications were observed. The only difference between the chemical systems used in experiments with HBr and DBr was the presence of D_2O in the latter case. This suggested that the addition of water in the reactor could be used in the case of the HBr reaction with OH and OD to minimize the wall effects due to the adsorption of HBr. This was verified, since reproducible kinetics were obtained for both reactants, OH (OD) and HBr, when H_2O was added into the reactor. Consequently, the low temperature measurements of k_1 and k_3 (see Tables 1 and 2) were carried out in the presence of water.

In a first series of experiments, the rate constants k_1 and k_3 were derived from the kinetics of OH and OD decay in excess of HBr, respectively. The configuration used for the introduction of the reactants into the reactor is shown in Fig. 1. H (D) atoms, formed in a microwave discharge (inlet 2), were introduced into the reactor through the outer tube of the movable injector. NO_2 was passed through the fixed inlet 3 and the second reactant (HBr) was injected through inlet 1. H_2O (when added) was flowed into the reactor together with HBr. The concentration of H_2O was generally in the range $(5–10) \times 10^{13}\ cm^3$ per molecule. It was determined using titration reaction $F + H_2O$ with an excess of

Table 1
Reaction OH + HBr → Br + H_2O (1): experimental conditions and results

N/exp[a]	T (K)	$([OH]_0/10^{12})$[b]	$([HBr]_0/10^{13})$[b]	k_1[c]	$\pm H_2O$[d]
8	360	0.5–1.0	0.3–4.1	0.97 ± 0.14	–
9	328	0.5–1.0	0.2–4.5	1.05 ± 0.12	–
9	298	0.5–0.7	0.2–3.0	1.11 ± 0.12	–
7	278	3.4–28.7	≈0.1	1.20 ± 0.13	–
9	260	0.9–1.5	0.2–3.9	1.12 ± 0.13	+
8	243	0.7–1.5	0.2–4.5	1.20 ± 0.14	+
7	230	0.7–1.5	0.2–4.0	1.46 ± 0.17	+

[a] Number of kinetic runs.
[b] Concentrations are in molecule cm^{-3} units.
[c] Rate constants are in 10^{-11} cm^3 s^{-1} per molecule units; the error represents $1\sigma + 10\%$; all the results were obtained from OH decay kinetics in excess of HBr, except at $T = 278$ K, where excess of OH over HBr was used.
[d] Experiments with H_2O added into the reactor (+) and without H_2O addition (−) (see text).

Table 2
Reaction OD + HBr → Br + HOD (3): experimental conditions and results

N/exp[a]	T (K)	$([OD]_0/10^{12})$[b]	$([HBr]_0/10^{13})$[b]	k_3[c]	$\pm H_2O$[d]
9	360	0.4–0.9	0.2–3.6	1.01 ± 0.13[e]	–
8	328	0.5–1.2	0.4–4.5	1.09 ± 0.12[e]	–
9	298	0.4–0.6	0.2–2.8	1.22 ± 0.14[e]	–
7	297	3.8–20.3	≈0.1	1.11 ± 0.12[f]	–
8	278	0.5–1.0	0.2–3.4	1.20 ± 0.17[e]	+
7	278	2.9–16.2	≈0.1	1.22 ± 0.13[f]	–
7	260	2.7–16.6	≈0.1	1.24 ± 0.16[f]	–
8	260	0.5–1.0	0.3–3.5	1.18 ± 0.15[e]	+
8	243	0.7–1.4	0.3–3.4	1.40 ± 0.16[e]	+
7	230	0.6–1.2	0.2–3.2	1.58 ± 0.21[e]	+

[a] Number of kinetic runs.
[b] Concentrations are in molecule cm^{-3} units.
[c] Rate constants are in 10^{-11} cm^3 s^{-1} per molecule units; the error $1\sigma + 10\%$.
[d] Experiments with H_2O added into the reactor (+) and without H_2O addition (−) (see text).
[e] Results from OD decay kinetics (in excess of HBr).
[f] Results from HBr decay kinetics (in excess of OD).

H_2O ($[F]_0 = \Delta[H_2O]$). The linear flow velocity in the reactor was in the range (1100–1600) cm s^{-1}. Br_2 in concentrations $(5–10) \times 10^{13}$ cm^3 per molecule was added at the downstream end of the reactor (inlet 4) for the indirect detection of OH and OD as HOBr and DOBr, respectively (see previous section). The kinetics of both reactants, OH (OD) and HBr, were monitored. It was observed, that under the present experimental conditions (summarized in Tables 1 and 2), the HBr concentration did not change significantly along the reactor, although in a few kinetic runs (at the lowest $[HBr]_0$), the HBr consumption could reach ≅ 10%. In these cases, the mean concentration of HBr along the reactor was used in the calculations. Examples of the exponential decay kinetics of OD in reaction (3) are shown in Fig. 3. Fig. 4 shows pseudo-first order rate constant, $k'_3 = k_3[HBr] + k_w$, as a function of the HBr concentration. k_w represents the rate of OH (OD) decay in the absence of HBr in the reactor and it was measured in separate experiments to be in the range (5–25) s^{-1} increasing with decreasing temperature. This

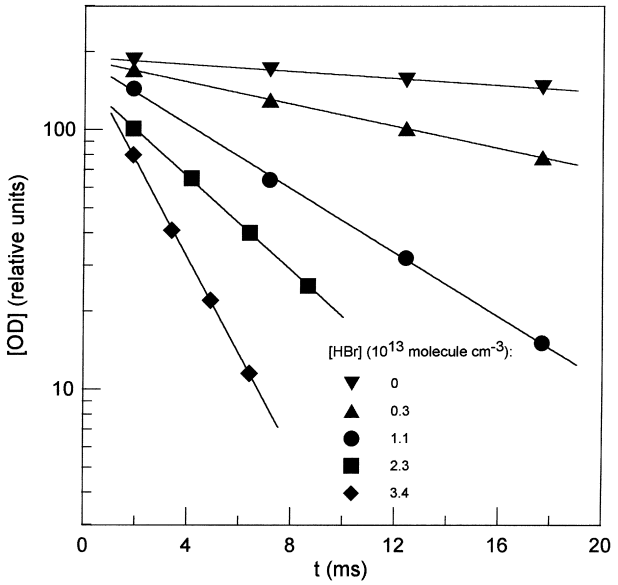

Fig. 3. Reaction OD + HBr → Br + HOD (3): example of experimental OD decay kinetics monitored in excess of HBr at $T = 243$ K.

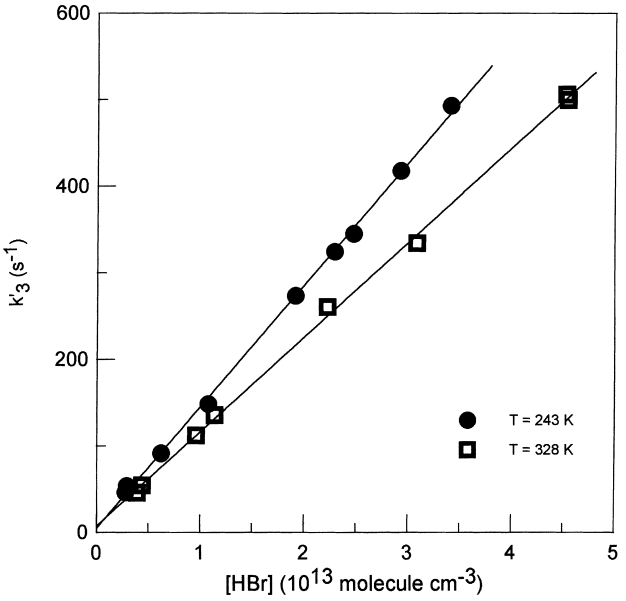

Fig. 4. Reaction OD + HBr → Br + HOD (3): example of pseudo-first order plots obtained from OD decay kinetics in excess of HBr.

decay rate of OH (OD) was due to the OH (OD) heterogeneous loss, to the reactions of OH (OD) with NO_2 (the NO_2 concentration in the reactor was in the range $(2–5) \times 10^{13}$ molecule cm^{-3}) and, to a less extent, to the OH (OD) disproportionation reactions (16) and (17):

$$OH + NO_2 (+M) \rightarrow HNO_3 (+M) \quad (14)$$

$k_{14} = 2.5 \times 10^{-30}$ $(T/300)^{-4.4}$ cm^6 s^{-1} per square molecule (for $M = N_2$) [11]

$$OD + NO_2 (+M) \rightarrow DNO_3 (+M) \quad (15)$$

$k_{15} = 1.27 \times 10^{-30}$ cm^6 s^{-1} per square molecule ($T = 298$ K, M = He) [26]

$$OH + OH \rightarrow O + H_2O \quad (16)$$

$k_{16} = 7.1 \times 10^{-13} \exp(210/T)$ cm^3 s^{-1} per molecule [17]

$$OD + OD \rightarrow O + D_2O \quad (17)$$

$k_{17} = 2.5 \times 10^{-13} \exp(170/T)$ cm^3 s^{-1} per molecule [17]

The value of k_{14} is recommended for M = N_2 [11], it can be lower by a factor 2 to 3 with He as a third body [27]. By comparison, the rate constant of the reaction of OD with NO_2 is: $k_{15} = 4.05 \times 10^{-30}$ and 1.27×10^{-30} cm^6 s^{-1} per square molecule for M = N_2 and He, respectively [24]. Finally, it can be noted that the zero intercepts of the pseudo-first order plots (Fig. 4) were always in good agreement with the values of k_w measured directly. All the measured values of k'_1 and k'_3 were corrected for axial and radial diffusion [28] of OH and OD. The diffusion coefficients for OH and OD in He were calculated from that for oxygen atoms $D_{O–He} = 0.9 \times (T/273)^{1.8}$ cm^2 s^{-1} (at 1 atm) [29]. The maximum correction was 20%. All the results obtained for k_1 and k_3 are summarized in Tables 1 and 2, respectively.

The measurements of k_1 showed no dependence upon the concentration of NO_2 ($[NO_2] = (1–5) \times 10^{13}$ molecule cm^{-3}) and H_2O, which was varied in the range $(0.1–1.0) \times 10^{14}$ molecule cm^{-3} (always in excess over HBr). In the case of reaction (3), the initial concentration of OD radicals was changed between 2.5×10^{11} and 4.2×10^{12} molecule cm^{-3}. k_3 was found to be insensitive to this variation. As noted in [8], HBr can be complexed with H_2O, leading to the formation of a species, which could react with OH. It seems that it was not the case in the present study. First, no signal was detected at $m/e = 98/100$ (H_2O–HBr^+). However, this could be expected even in the presence of this complex since it would have been dissociated by electron impact at the energy used (≈25 eV). Secondly, OH (OD) kinetics were independent of the H_2O concentration, which was widely changed (see above). Finally, the fact that the results obtained for k_1 and k_3 from the monitoring of HBr kinetics in excess of OH or OD (as shown below) were the same as those from the radicals consumption kinetics in excess of HBr, seems to show that the effect of an HBr–H_2O complex formation was negligible under the present experimental conditions.

In the second series of experiments, the rate constants of reactions (1) and (3) were derived from the kinetics of HBr consumption monitored in excess of OH or OD radicals. The configuration used for the introduction of the reactants was the same as above. OH and OD kinetics were monitored simultaneously with the HBr decay kinetics. Consumption of OH (OD) radicals from 20 to 40% was observed. In the calculation of the rate constants, [OH] and [OD] were kept constant (with a mean value along the HBr decay kinetics). A numerical simulation of the HBr decay kinetics, using the observed [OH] ([OD]) temporal profiles, gave the same values for k_1 and k_3 within ±5%. The ranges of the concentrations of OH and OD and of the initial concentrations of HBr are given in Tables 1 and 2. Fig. 5 shows typical pseudo-first order plots of HBr decay in reaction (3) with an excess of OD. All the measured values of k'_1 and k'_3 were corrected for axial and radial diffusion of HBr. The diffusion coefficient $D_{HBr–He}$ was calculated from $D_{Kr–He}$ [30]. The maximum correction was around 10%. The final results obtained for k_1 and k_3 in this series of experiments are given in Tables 1 and 2, respectively. These results are in good agreement with those measured in the previous series of experiments, where OH and OD kinetics were monitored in excess of HBr.

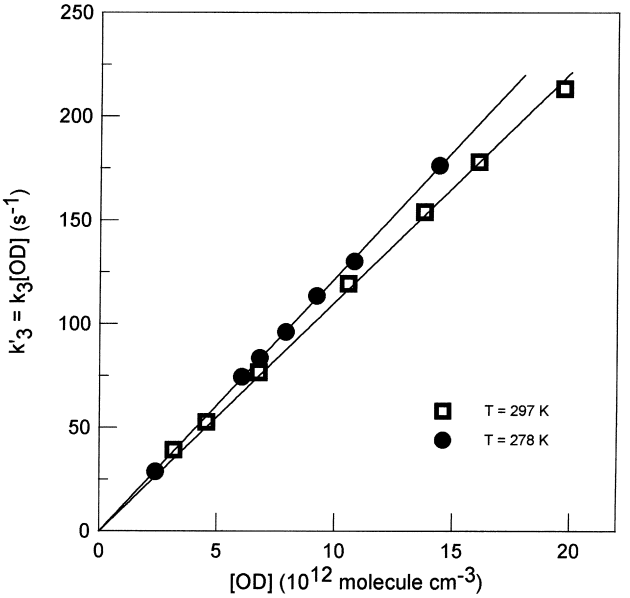

Fig. 5. Reaction OD + HBr → Br + HOD (3): example of pseudo-first order plots obtained from HBr decay kinetics in excess of OD radicals.

Since relatively high concentrations of OH and OD were used in these experiments, leading to O atom formation in the disproportionation reactions of OH (16) and OD (17), the contribution of O + HBr reaction to measured HBr decays should be estimated:

$$O + HBr \rightarrow OH + Br \quad (18)$$

$k_{18} = 5.8 \times 10^{-12} \exp(-1500/T)$ cm^3 s^{-1} per molecule [11].

Taking into account the relatively low value of k_{18} and that oxygen atoms are consumed in reactions (19) with OH and (20) with NO_2, the contribution of reaction (18) to the HBr decay can be considered as negligible compared to reaction (1):

$$O + OH \rightarrow H + O_2 \quad (19)$$

$k_{19} = 2.2 \times 10^{-11} \exp(120/T)$ cm^3 s^{-1} per molecule [11]

$$O + NO_2 \rightarrow NO + O_2 \quad (20)$$

$k_{20} = 6.5 \times 10^{-12} \exp(120/T)$ cm^3 s^{-1} per molecule [11].

The same conclusion was drawn for the OD + HBr reaction, since the OD + OD reaction, producing O atoms,

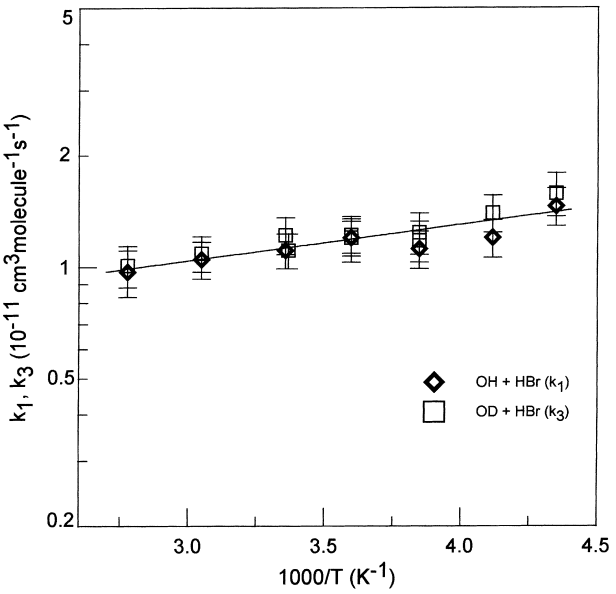

Fig. 6. Temperature dependence of the rate constants of HBr reactions with OH and OD.

has a rate constant around 3.5 times lower than that of the OH + OH reaction [17].

It was also concluded that the possible contribution of the heterogeneous reaction of OH (OD) with HBr was negligible under the present experimental conditions. This was supported by the good agreement between the results obtained under different conditions: in excess of HBr over OH (OD) and in excess of the radicals over HBr. Moreover, an excellent agreement can be noted between the results obtained for k_1 at low temperatures in the present study and in that of Ravishankara et al. [8] (see Section 4), where the laser flash photolysis-resonance fluorescence technique (free of heterogeneous complication) was employed.

All the kinetic results obtained in this work by the two methods are also presented in Fig. 6, which shows the temperature dependence of both k_1 and k_3. As can be seen from Tables 1 and 2 and from Fig. 6, the values measured for k_1 and k_3 are indistinguishable within the experimental uncertainty. That is why all the experimental data for k_1 and k_3 were fitted together and finally the same Arrhenius expression is given for both rate constants:

$k_1 \approx k_3 = (5.3 \pm 1.2) \times 10^{-12} \exp\{(225 \pm 60)/T\}$ cm^3 s^{-1} per molecule.

The quoted uncertainties represent two standard deviations.

3.2. Reactions OH + DBr (4) and OD + DBr (5)

The rate constants of the DBr reactions with OH and OD radicals were measured under pseudo-first order conditions, using an excess of DBr over the radicals:

$$OH + DBr \rightarrow Br + HOD$$

$$OD + DBr \rightarrow Br + D_2O$$

The configuration used for the introduction of the reactants was the same as shown above for the HBr reaction with OH and OD. DBr was introduced into the reactor by flowing helium through a reservoir containing a liquid DBr/D_2O mixture. The initial concentrations of OH and OD radicals were in the range $(0.4–1.0) \times 10^{12}$ molecule cm^{-3}. The ranges of HBr concentrations used in these series of experiments are shown in Tables 3 and 4. The linear flow velocity in the reactor was (1300–1550) cm s^{-1}. The concentration of D_2O in the reactor was measured to be a few times that of DBr. The kinetics of both OH (OD) and DBr were monitored. It was observed that DBr consumption was negligible under the experimental conditions used (Tables 3 and 4). The procedure employed for the treatment of the experimental data was similar to that for HBr reactions (1) and (3). Pseudo-first order rate constants were derived from the exponential decay kinetics of the radicals and were plotted as a function of the concentration of the excess reactant DBr. The values of the rate constants k_4 and k_5 were determined from the slopes of these pseudo-first order plots. Final results obtained in this way for k_4 and k_5 are shown in Tables 3 and 4 and in Fig. 7. Again, within the experimental uncertainty, the same values of the rate constants were found for the DBr + OH and DBr + OD reactions. The line in Fig. 7 represents an exponential fit to all the data obtained for k_4 and k_5, yielding the following Arrhenius expression:

$k_4 \approx k_5 = (4.3 \pm 1.2) \times 10^{-12} \exp\{(125 \pm 80)/T\}$ cm^3 s^{-1} per molecule

No evidence for heterogeneous complications (even at the lowest temperatures of the study) was observed in this series of experiments. The OH (OD) kinetics were always reproducible, the concentration of DBr being changed in a random order from one kinetics to another. The rates of the OH (OD) decays measured in the absence of DBr in the reactor, prior to and just after the experiments on OH (OD) + DBr reactions were always in good agreement. Besides, the values of the zero intercepts of the pseudo-first order plots were always consistent with the OH (OD) loss rate measured separately in the absence of DBr.

3.3. Isotope exchange reaction OD + HBr → OH + DBr (3′) and OH + DBr → OD + HBr (4′)

In the previous sections, only one reactive channel forming HOD and Br atoms is considered for both reactions (3) and (4). Another possible channel is the H/D atom exchange reaction:

$$OD + HBr \rightarrow OH + DBr \quad (3')$$

$$OH + DBr \rightarrow OD + HBr \quad (4')$$

In order to estimate the branching ratio for channels (3′) and (4′), additional experiments were performed, consisting of chemical titration of relatively high concentrations of OD and OH by an excess of HBr and DBr, respectively, with subsequent detection of DBr and HBr possibly formed in

Table 3
Reaction OH + DBr → Br + HOD (4): experimental conditions and results

N/exp[a]	*T* (K)	[DBr] (10^{13} molecule cm^{-3})	k_4[b] (10^{-11} cm^3 s^{-1} per molecule)
10	360	0.3–6.6	0.60 ± 0.07
8	328	0.3–6.4	0.57 ± 0.07
11	296	0.3–5.1	0.59 ± 0.09
7	278	0.4–6.2	0.64 ± 0.08
9	260	0.5–4.9	0.68 ± 0.08
7	230	0.2–1.6	0.74 ± 0.11

[a] Number of kinetic runs.
[b] Quoted uncertainty represents $1\sigma + 10\%$.

Table 4
Reaction OD + DBr → Br + D_2O (5): experimental conditions and results

N/exp[a]	*T* (K)	[DBr] (10^{13} molecule cm^{-3})	k_5[b] (10^{-11} cm^3 s^{-1} per molecule)[b]
8	360	0.3–5.7	0.63 ± 0.09
8	328	0.3–6.1	0.66 ± 0.09
8	300	0.4–5.7	0.72 ± 0.11
11	278	0.5–7.0	0.77 ± 0.10
9	260	0.2–6.3	0.71 ± 0.10
9	243	0.2–3.4	0.74 ± 0.11
6	230	0.4–1.5	0.72 ± 0.09

[a] Number of kinetic runs.
[b] Quoted uncertainty represents $1\sigma + 10\%$.

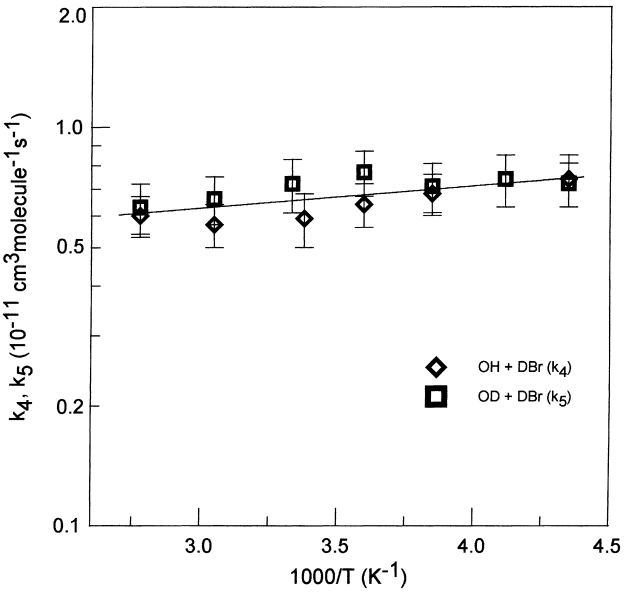

Fig. 7. Temperature dependence of the rate constants of DBr reactions with OH and OD.

reactions (3′) and (4′). The experiments were carried out at $T = 298$ K. As in the above experiments, OH and OD radicals were generated through reactions of H and D atoms with NO_2, respectively. In order to obtain higher concentrations of the radicals, the source reactions (6) and (7) took place directly in the reactor itself, H and D atoms being introduced through inlet 1 of the movable injector and NO_2 through inlet 3. The titrating excess reactants HBr and DBr were flowed into the reactor through inlet 4. In order to measure the initial concentrations of OD and OH, Br_2 was added into the reactor through inlet 4 instead of HBr and DBr.

In the case of the OH reaction with DBr, it was observed that for the highest OH concentration (3.3×10^{13} molecule cm^{-3}) totally consumed in the reaction with DBr, the concentration of HBr formed was less than 1.5×10^{11} molecule cm^{-3}. This allowed for the determination of an upper limit for the branching ratio of HBr forming channel in reaction (4):

$$\frac{k_4'}{k_4} < 0.005.$$

One may note that the measurements of the small HBr signals in this case were complicated by the observed contribution of DBr (high concentrations of DBr were used to provide a rapid complete titration of OH) to the signals at $m/e = 80$ and 82.

In the case of the OD reaction with HBr, a signal at $m/e = 83$ (which can be attributed to DBr) was observed. In fact, this signal may have the different origins. It was not tried to quantify possible secondary sources of DBr. In order to evaluate the rate of DBr formation in reaction (3′), the initial concentration of OD was varied from 6×10^{12} to 6×10^{13} molecule cm^{-3}. Only a slight increase of the signal at $m/e = 83$ was observed when [OD] was changed in this concentration range. If this increase is totally attributed to the formation of DBr, it corresponds to an increase of the DBr concentration of less than 5×10^{11} molecule cm^{-3}. Thus, an upper limit for the DBr formation channel (3′) can be derived:

$$\frac{k_3'}{k_3} < 0.01$$

Table 5
Summary of the data for the rate constant of the reaction OH + HBr → H_2O + Br at 295–298 K

k_1 (10^{-11} cm^3 s^{-1} per molecule)	Method[a]	Reference
0.51 ± 0.09	DF/EPR	Takacs and Glass [2]
0.45 ± 0.10	FP/UVA	Smith and Zellner [3]
1.19 ± 0.14	FP/RF	Ravishankara et al. [8]
0.60 ± 0.03	FP/RF	Husain et al. [4]
0.92 ± 0.07	DF/EPR	Jourdain et al. [5]
1.12 ± 0.05	FP/LIF	Cannon et al. [6]
1.1 ± 0.1	FP/LIF + RF	Ravishankara et al. [7]
1.16 ± 0.04	FP/LIF	Sims et al. [9]
1.1 ± 0.2	Revue	JPL-97 [11]
1.1 ± 0.1	Revue	IUPAC-97 [12]
1.1 ± 0.1	DF/MS	This work

[a] DF/EPR: discharge flow system/electron paramagnetic resonance; FP/UVA: flash photolysis/UV absorption; FP/RF: flash photolysis/resonance fluorescence; FP/LIF: flash photolysis/laser induced fluorescence; DF/MS: discharge flow system/mass spectrometry.

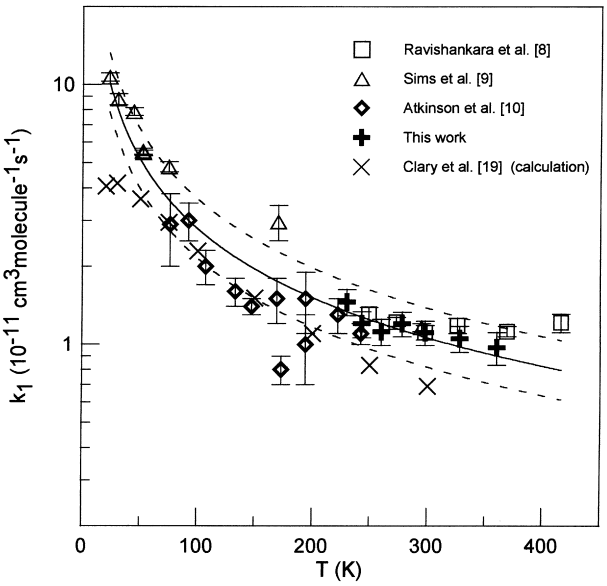

Fig. 8. Reaction OH + HBr → Br + H_2O (1): summary of the results from the temperature dependence studies of the reaction (see text).

4. Discussion

The results obtained for the rate constant of the OH + HBr reaction can be compared with those from previous studies. A summary of the room temperature data for k_1 is presented in Table 5. As one can see, the value of k_1 measured in this study agrees well with those from most recent studies [6,7,9] and with the currently recommended ones [11,12]. The temperature dependence of the rate constant of reaction (1) has been studied for a first time in [8], where k_1 was found to be independent of temperature with the average value of $k_1 = (1.19 \pm 0.14) \times 10^{-11}$ cm^3 s^{-1} per molecule at $T = 249-416$ K. In another study [9], the monotonic increase of the rate constant with decreasing temperature from 295 to 23 K was reported. Finally, the most recent study of the reaction (1) [10], using a pulsed supersonic flow reactor combined with LIF detection of OH was used, supports the temperature dependence of k_1, observed in [9], however only below 150 K. On the contrary, a temperature independent value of $k_1 = (1.2 \pm 0.2) \times 10^{-11}$ cm^3 s^{-1} per molecule was recommended in [10] for the temperatures throughout 'the terrestrial atmosphere'. Fig. 8 presents (as $\ln k_1 = f(T)$ as in [10]) a summary of the results for k_1 from all available temperature dependence studies, including this one. The present results obtained at $T = 230$–360 K are in good agreement with those from previous study [8], conducted in a similar temperature range, except that a distinct, although slight, negative temperature dependence of k_1 is observed in the present study. It can be noted also that the data from [8] show a small increase in k_1 at $T = 298$–249 K. Sims et al. [9] have shown that their own results for k_1 (at $T = 23$–295 K) together with those from [8] at $T = 298$–249 K can be fitted with the expression: $k_1 = (1.26 \pm 0.24) \times 10^{-11}$ $(T/298)^{-0.86 \pm 0.10}$ cm^3 s^{-1} per molecule. We have repeated this procedure here using the data from all previous studies [8–10] and the present one. The solid line in Fig. 8 shows the resulting fit and corresponds to the expression:

$k_1 = 1.07 \times 10^{-11}$ $(T/298)^{-0.88}$ cm^3 s^{-1} per molecule

The dashed lines represent ±30% deviation from the above expression and show that almost all the existing data on $k_1(T)$ at $T = 23$–370 K can be represented by this expression with the uncertainty factor 1.3 (this uncertainty factor is lower at temperatures between 230 and 300 K). For comparison, currently recommended values of $k_1(T)$ are: 1.1×10^{-11} $(T/298)^{-0.8}$ (200–400 K) [12] and $1.1 \times 10^{-11} \exp\{(0 \pm 250)/T\}$ cm^3 s^{-1} per molecule [11].

A theoretical calculation of the OH + HBr reaction rate has been attempted in [18], where the adiabatic capture approximation has been applied to estimate the rate constant of this reaction. This method only provides an upper limit for the rate constant and at very low temperatures. The value of this upper limit for k_1 was calculated to be 3.5×10^{-10} cm^3 s^{-1} per molecule at $T = 20$ K [18], i.e. about a factor 3 higher than the experimental value of [9]. In another theoretical study [19], quantum scattering calculations with use of rotating bond approximation method (RBA) have been performed to describe the dependence of k_1 on temperature. Results of these calculations are shown in Fig. 8 along with the experimental data. It is seen that the negative temperature dependence of k_1 is reproduced by this model. In the same study, a simple explanation of the negative temperature dependence of k_1 was proposed. The computed reactive cross-sections were found to have $(2J + 1)^{-1}$ dependence on the OH rotational quantum number J. This strong rotational effect was shown to be responsible $T^{-1/2}$ dependence of the rate constant [19]:

$$k(T) \approx k_0(T)\sqrt{\frac{B\pi}{k_B T}} \quad \text{(I)}$$

where $k_0(T)$ is the rate constant for OH ($J = 0$), B is the rotational constant of OH and k_B is the Boltzman constant. Assuming that the temperature dependence of $k_0(T)$ arises mainly from the electronic partition function of OH, the simple formula for the rate constant was obtained [19]: $k(T) = AT^{-1/2}[1 + \exp(-181/T)]^{-1}$ (A is a parameter). This simplified expression fits well the ultra-low temperature k_1 data [9,19], however is not operative at higher temperatures.

To our knowledge, only one of the isotopic variants of reaction (1), the OH + DBr reaction, has been investigated in only one previous study [4]. The value of $k_4 = (2.05 \pm 0.14) \times 10^{-12}$ cm^3 s^{-1} per molecule was obtained at $T = 300$ K using the flash photolysis technique with resonance fluorescence for OH detection. This value is lower than that measured in the present work by a factor around 3. The k_4 value of [4] may be considered as underestimated since the value of $k_1 = (6.01 \pm 0.32) \times 10^{-12}$ cm^3 s^{-1} per molecule, measured in that study was also lower (by a factor of 2) than the values currently recommended and measured in the present work. The kinetic isotope effect (KIE) ($k_1/k_4 \approx 2.9$ at $T = 300$ K) observed in [4] also differs from that measured here ($\approx$1.7 at room temperature). The origin of the discrepancy between the two values of k_4 (from this work and [4]) as well as between different measurements of k_1 (Table 5), is very likely linked to the procedure for the determination of the HBr absolute concentrations in the different studies, as previously suggested [7].

As shown above, the rate constants for the reactions (1), (3)–(5) were found to be the same within the limits of the experimental uncertainty, i.e. negligible secondary kinetic isotope effect was observed in the present study: $k_1/k_3 \approx k_4/k_5 \approx 1$ (within 15% experimental uncertainty). In [31], the vibrational excitation of H_2O and HOD formed in the reactions (1) and (3), respectively, was analyzed using the infrared emission technique. From the comparison of the relative H_2O and HOD emission intensities the ratio k_1/k_3 was found to be 1.3 ± 0.2. This value, although somewhat higher, is consistent with the present observation within quoted uncertainty limits. It is interesting to compare the kinetic isotope effect data for reaction (1) with those for analogous reaction of OH radicals with HCl. This reaction and all its isotopic analogs have been studied in [32] and more recently in [33]:

$$OH + HCl \rightarrow Cl + H_2O \quad (21a)$$

$$OD + HCl \rightarrow Cl + HOD \quad (21b)$$

$$OH + DCl \rightarrow Cl + HOD \quad (21c)$$

$$OH + DCl \rightarrow Cl + D_2O \quad (21d)$$

The secondary kinetic isotope effect observed in these studies at $T = 298$ K was: $k_{21a}/k_{21b} = 1.55$ [32], 0.93 [33] and $k_{21c}/k_{21d} = 0.85$ [32], 0.93 [33]. Although in the present study the values of k_3 and k_1 were considered to be the same, a slightly higher value of k_3 compared to k_1 was observed in the whole temperature range used (see Tables 1 and 2 and Fig. 6). A similar picture was observed for reactions (4) and (5). These observations are very similar to those from [33] for reaction (21). It can be noted also, that usually OH and OD have the same rate coefficients for exothermic hydrogen-abstraction reactions as it was observed, for example, for the reactions of OH with H_2O_2 [34], CH_3OOH [35], H_2 [36], n-C_4H_{10} [37] and HI [31]. The primary kinetic isotope effect observed for OH + HCl reaction, $k_{21a}/k_{21c} = 6.2$ [32], 3.08 [33] and $k_{21b}/k_{21d} = 3.4$ [32], 3.06 [33] is higher than that found here for reaction (1): $k_1/k_4 \approx k_3/k_5 \approx 1.7$. From another side, the KIE measured in [3,4], $k_{21a}/k_{21c} = 2.0$ [3] and $k_{21a}/k_{21c} = 1.9$ [4], are very close to the present observation for reaction (1).

Extensive quasiclassical trajectory (QCT) calculations were performed [20] in order to study the dynamics of the OH and OD reactions with HBr on an empirical potential energy surface (PES). The values of the rate constants k_1, k_3 and k_4 calculated by this method as well as those using variational transition state theory (VTST) were compared with the available experimental data. The experimental value of k_3 used in [20] for comparison with the calculations was estimated by analogy with the reaction OD + HCl [32], and k_4 was calculated from known k_1 [11] and $k_1/k_4 = 2.93$ reported in [4]. The present direct measurements of the rate constants for all isotope analogs of the reaction (1) provide an experimental base for comparison with theory. Table 6, summarizing the results of the calculations, is reproduced from [20], except that experimental results were replaced by those from the present work. A first feature is that the values

Table 6
Experimental rate constants (this study) and calculated ones [20] for reactions (1), (3) and (4) at $T = 300$ K

Model	Rate constant (10^{-11} cm^3 s^{-1} per molecule)
OH + HBr (1)	
Experimental[a]	1.12 ± 0.17
VTST (Clary potential[b])	1.04
VTST (Modified potential[c])	0.54
RBA (Clary potential) [19]	0.7
QCT (Clary potential)	2.4
QCT (Modified potential)	1.6
OD + HBr (3)	
Experimental	1.12 ± 0.17
VTST (Clary potential)	1.3
VTST (Modified potential)	0.75
QCT (Clary potential)	2.1
OH + DBr (4)	
Experimental	0.65 ± 0.10
VTST (Clary potential)	1.22
VTST (Modified potential)	0.71

[a] Calculated from the $k(T)$ Arrhenius expressions obtained in the present study with addition of the 15% conservative error.

[b] Clary potential: PES formulated by Clary et al. [19], based on accurate H_2O potential and on transition state for OH + HCl reaction.

[c] Modified potential: PES from [19] with parameters adjusted to fit the experimentally measured H_2O vibrational energy and the thermal rate constant [20].

of the rate constants calculated by various computational methods are close to the experimental results. However, the comparison of the kinetic isotope effect calculated within the same computational method with that from experiments seems to be more appropriate for the theory testing. As can be seen, the variational transition state calculations give a small inverse secondary KIE ($k_3/k_1 = 1.25$–1.40), which is in agreement with the experimental observation of $k_3 \geq k_1$. On the contrary, the primary kinetic isotope effect measured here, $k_1/k_4 \approx k_3/k_5 \approx 1.7$, clearly disagrees with the calculated one. The calculated VTST rate constant for OH + DBr reaction for both potential energy surfaces is ≈20% larger than for reaction (1). In [20], the ratio $k_1/k_4 = 2.93 \pm 0.25$ [4] was used for comparison with the calculated results. It was noted, that such a large ratio of the rate constants is difficult to explain by the transition state theory, if transition states are located early in the entrance channel, because the HBr and DBr frequencies are similar in the reactant and transition state. Requirement of new experimental measurements of the primary KIE to provide constraints to the entrance channel part of PES was pointed out [20]. The present study supplies such data for a range of temperature (230–360) K and, in addition, it shows that the experimental k_1/k_4 ratio is significantly lower than that considered in [20] for comparison.

The upper limits for the branching ratios of the isotope exchange channels (3′) and (4′) were measured in the present study to be: $k_{3'}/k_3 < 0.01$ and $k_{4'}/k_4 < 0.005$. Combining these branching ratios with the data obtained above for k_3 and k_4, one can derive the upper limits for the rate constants of reactions (3′) and (4′) at $T = 298$ K: $k_{3'} < 1 \times 10^{-13}$ and $k_{4'} < 3 \times 10^{-14}$ cm^3 s^{-1} per molecule. These results seem to be reasonable, especially if compared with known data for similar reactions of hydroxyl radicals:

$$OH + D_2O \rightarrow OD + HOD \quad (22)$$

$$OD + H_2O \rightarrow OH + HOD \quad (23)$$

$$OD + H_2O_2 \rightarrow OH + HOOD \quad (24)$$

Reactions (22) and (23), studied recently [38], have been shown to be slow. The values of the rate constants measured at T=300 K were: $k_{22} < 5 \times 10^{-17}$ and $k_{23} = (3.0 \pm 1.0) \times 10^{-16}$ cm^3 s^{-1} per molecule. Similar result for reaction (23) was obtained [35], where the upper limit for k_{23} was reported: $k_{23} < 2 \times 10^{-15}$ ($T = 249$ K) and $<2 \times 10^{-14}$ cm^3 s^{-1} per molecule ($T = 423$ K). The isotope exchange reaction (24) is also slow with an upper limit of the rate constant at 273 K: $k_{24} < 22 \times 10^{-15}$ cm^3 s^{-1} per molecule [34].

In conclusion, new kinetic data have been provided by the present study. A negative temperature dependence of the rate constant of the reaction OH + HBr, previously observed at ultra-low temperatures, was shown to be valid up to 360 K and new data were obtained for the isotopic analogs of reaction (1). This kinetic information can be useful to better define the role of the OH + HBr reaction at the lowest temperatures of the stratosphere and as a testing ground for theoretical calculations of reaction rates.

Acknowledgements

This study has been carried out within a project funded by the European Commission within the ‘Environment and Climate’ Programme (contract ENV - CT97 - 0576).

References

[1] R.P. Wayne, Chemistry of the Atmosphere, Oxford University Press, Oxford, 1991.
[2] G.A. Takacs, G.P. Glass, J. Phys. Chem. 77 (1973) 1060.
[3] I.W.M. Smith, R. Zellner, J. Chem. Soc. Faraday Trans. 2 70 (1974) 1045.
[4] D. Husain, J.M. Plane, N.K.H. Slater, J. Chem. Soc. Faraday Trans. 2 77 (1981) 1949.
[5] J.L. Jourdain, G. Le Bras, J. Combourieu, Chem. Phys. Lett. 78 (1981) 483.
[6] B.D. Cannon, J.S. Robertshaw, I.W.M. Smith, M.D. Williams, Chem. Phys. Lett. 105 (1984) 380.
[7] A.R. Ravishankara, P.H. Wine, J.R. Wells, J. Chem. Phys. 83 (1985) 447.
[8] A.R. Ravishankara, P.H. Wine, A.O. Langford, Chem. Phys. Lett. 63 (1979) 479.
[9] I.R. Sims, I.W.M. Smith, D.C. Clary, P. Bocherel, B.R. Rowe, J. Chem. Phys. 101 (1994) 1748.
[10] D.B. Atkinson, V.I. Jaramillo, M.A. Smith, J. Phys. Chem. A 101 (1997) 3356.
[11] W.B. De More, S.P. Sander, D.M. Golden, R.F. Hampson, M.J. Kurylo, C.J. Howard, A.R. Ravishankara, C.E. Kolb, M.J. Molina, Chemical Kinetics and Photochemical Data for Use in Stratospheric Modeling NASA, JPL, California Institute of Technology, Pasadena, CA, 1997.
[12] R. Atkinson, D.L. Baulch, R.A. Cox, R.F. Hampson, J.A. Kerr, M.J. Rossy, J. Troe, J. Phys. Chem. Ref. Data 26 (1997) 521.
[13] M.P. Chipperfield, D.E. Shallcross, D.J. Lary, Geophys. Res. Lett. 24 (1997) 3025.
[14] D.J. Chartland, L.C. McConnell, Geophys. Res. Lett. 25 (1998) 55.
[15] D.J. Bogan, R.P. Thorn, F.L. Nesbitt, L.J. Stief, J. Phys. Chem. 100 (1996) 14838.
[16] Y. Bedjanian, G. Le Bras, G. Poulet, Int. J. Chem. Kinet. (1999), in press.
[17] Y. Bedjanian, G. Le Bras, G. Poulet, J. Phys. Chem. A 103 (1999) 7017.
[18] D.C. Clary, T.S. Stoecklin, A.G. Wickham, J. Chem. Soc. Faraday Trans. 89 (1993) 2185.
[19] D.C. Clary, G. Nyman, R. Hernandez, J. Chem. Phys. 101 (1994) 3704.
[20] B. Nizamov, D.W. Setser, H. Wang, G.H. Peslherbe, W.L. Hase, J. Chem. Phys. 105 (1996) 9897.
[21] M.K. Gilles, J.B. Burkholder, A.R. Ravishankara, Int. J. Chem. Kinet. 31 (1999) 417.
[22] J.M. Nicovich, C.A. van Dijk, K.D. Kruetter, P.H. Wine, J. Phys. Chem. 95 (1991) 9890.
[23] P.W. Seakins, M.J. Pilling, J.T. Niiranen, D. Gutman, L.N. Krasnoperov, J. Phys. Chem. 96 (1992) 9847.
[24] Y. Wada, T. Takayanagi, H. Umemoto, S. Tsunashima, S. Sato, J. Chem. Phys. 94 (1991) 4896.
[25] H. Umemoto, Y. Wada, S. Tsunashima, Chem. Phys. 143 (1990) 333.

[26] A.R. Bossard, D.L. Singleton, G. Paraskevopoulos, Int. J. Chem. Kinet. 20 (1988) 609.
[27] W.G. Mallard, F. Westley, J.T. Herron, D. Frizzell, R.F. Hampson, NIST Chemical Kinetics Data Base, ver. 1 7-2Q98, NIST Standard Reference Data, Gaithersburg, MID, 1998.
[28] F. Kaufman, J. Phys. Chem. 88 (1984) 4909.
[29] V.V. Zelenov, A.S. Kukui, A.F. Dodonov, Sov. J. Chem. Phys. 5 (1990) 1109.
[30] T.R. Morrero, E.A. Mason, J. Phys. Chem. Ref. Data 1 (1972) 3.
[31] N.I. Butkovskaya, D.W. Setser, J. Chem. Phys. 106 (1997) 5028.
[32] I.W.M. Smith, M.D. Williams, J. Chem. Soc. Faraday Trans. 2 82 (1986) 1043.
[33] F. Battin-Leclerc, I.K. Kim, R.K. Talukdar, R.W. Portmann, A.R. Ravishankara, R. Steckler, D. Brown, J. Phys. Chem. 103 (1999) 3237.
[34] G.L. Vaghjiani, A.R. Ravishankara, N. Cohen, J. Phys. Chem. 93 (1989) 7833.
[35] G.L. Vaghjiani, A.R. Ravishankara, J. Phys. Chem. 93 (1989) 1948.
[36] R.K. Talukdar, T. Gierczak, L. Goldfarb, Y. Rudich, B.S. Madhara Rao, A.R. Ravishankara, J. Phys. Chem. 100 (1996) 3037.
[37] G. Paraskevopoulos, W.S. Nip, Can. J. Chem. 58 (1980) 2146.
[38] M.K. Dubey, R. Mohrschladt, N.M. Donahue, J.G. Anderson, J. Phys. Chem. A 101 (1997) 1494.